# Presacral Masses: Multimodality Imaging of a Multidisciplinary Space[1]

*Kendra S. Hain, MD • Perry J. Pickhardt, MD • Meghan G. Lubner, MD*
*Christine O. Menias, MD • Sanjeev Bhalla, MD*

**ONLINE-ONLY SA-CME**

*See www.rsna.org/education/search/RG*

**LEARNING OBJECTIVES**

*After completing this journal-based SA-CME activity, participants will be able to:*

- Describe the anatomic boundaries of the presacral space.
- List the major categories of space-occupying masses in the presacral space on the basis of their origin.
- Discuss how to formulate a systematic differential diagnosis for presacral masses on the basis of imaging findings.

**TEACHING POINTS**

*See last page*

The presacral space is a clinically important space that is relevant to multiple disciplines and lies at the intersection of the axial skeleton, neural axis, and pelvic soft tissues. A wide variety of benign and malignant conditions may derive from its various elements. An appropriate differential diagnosis may be formulated from a more comprehensive list by considering the specific imaging features of a given case: In particular, involvement of the sacrum (either remodeling or destruction) and the presence or absence of a solid, soft-tissue component may help narrow the differential diagnosis. Typically, osteochondral and neurogenic tumors remodel or destroy the sacrum, whereas sacral involvement is less common in patients with a mesenchymal tumor. Ewing sarcomas and chordomas are typically associated with a large soft-tissue mass. Demographic features are also important: Typically, congenital and developmental tumors occur in younger patients, and chondrosarcomas occur in older patients (mean age, 45 years). Finally, specific imaging features may help establish the diagnosis. For instance, an osseous or chondroid matrix is indicative of osteosarcoma or chondrosarcomas; neurofibromas may have a target appearance at magnetic resonance (MR) imaging; hemangiomas have areas of increased signal intensity on T1-weighted MR images, a result of fat and hemorrhage; and myeloplipomas contain macroscopic fat.

## Introduction

The presacral space is a clinically important space that is relevant to multiple disciplines. It lies at the intersection of the axial skeleton, neural axis, and soft tissues of the pelvis. Its anatomic boundaries include the rectum anteriorly; the presacral fascia, sacrum, and coccyx posteriorly; and the levator ani inferiorly (Fig 1). The presacral fascia extends inferiorly and separates the presacral space from the supralevator space (1). The presacral space is bounded by the pelvic peritoneal reflection superiorly and the iliac vessels and ureters laterally. Its contents include osteochondral tissue from the sacrum and coccyx, neural tissue from the cauda equina and branches of the sacral plexus, and mesenchymal tissue from adjacent

**Abbreviations:** CSF = cerebrospinal fluid, NF1 = neurofibromatosis type 1

**RadioGraphics 2013;** 33:1145–1167 • **Published online** 10.1148/rg.334115171 • **Content Codes:** GI GN GU MR

[1]From the Department of Radiology, University of Wisconsin School of Medicine and Public Health, E3/311 Clinical Science Center, 600 Highland Ave, Madison, WI 53792-3252 (K.S.H., P.J.P., M.G.L.); and Mallinckrodt Institute of Radiology, Washington University School of Medicine, St Louis, Mo (C.O.M., S.B.) Presented as an education exhibit at the 2009 RSNA Annual Meeting. Received November 9, 2011; revision requested April 27, 2012, and received August 10; final version accepted October 22. For this journal-based SA-CME activity, the author P.J.P. has disclosed financial relationships (see p 1166); the other authors, editor, and reviewers have no relevant relationships to disclose. **Address correspondence to** P.J.P. (e-mail: *ppickhardt2@uwhealth.org*).

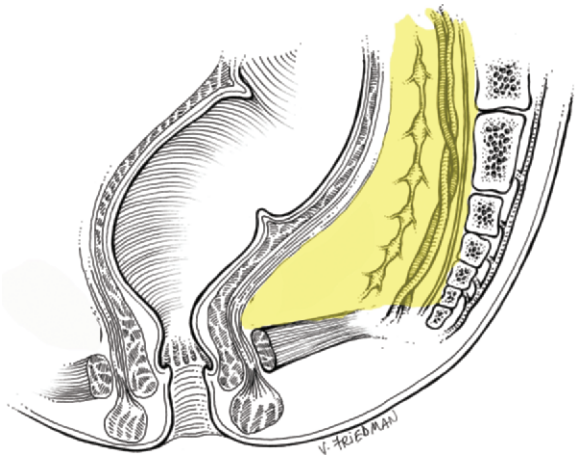

**Figure 1.** The presacral space. Illustration shows the presacral space (yellow area), which is bordered by the rectum anteriorly; the pelvic peritoneal reflection superiorly; the levator ani muscles inferiorly; and the presacral fascia, sacrum, and coccyx posteriorly. The lateral margins are demarcated by the iliac vessels and ureters. This space is bordered by and contains a variety of different tissue components that may give rise to a wide array of conditions.

**Table 1**
**Presacral Masses Encountered at Imaging**

| Origin | Mass |
|---|---|
| Osteochondral | |
| Benign | Osteoma, simple bone cyst, aneursmal bone cyst, giant cell tumor |
| Malignant | Ewing sarcoma, osteosarcoma, chondrosarcoma |
| Neurogenic | |
| Benign | Neurofibroma, ependymoma, neuroblastoma, schwannoma, dural ectasia, anterior sacral meningocele |
| Malignant | Neurofibrosarcoma, chordoma, malignant schwannoma |
| Mesenchymal | |
| Benign | Hemangioma, fibroma or fibrosis, myelolipoma, solitary fibrous tumor, Castleman disease |
| Malignant | Soft-tissue sarcoma, lymphoma, gastrointestinal stromal tumor |
| Metastatic disease | Epithelial malignancies |
| Unknown | Desmoplastic small round-cell tumor |
| Congenital or developmental | |
| Benign | Retrorectal cystic hamartoma, rectal duplication cyst, epidermoid cyst, dermoid cyst |
| Malignant | Teratocarcinoma, teratoma, yolk sac tumor |
| Other | Infectious, inflammatory, posttraumatic |

organs, as well as surrounding connective tissue and blood and lymphatic vessels. A wide variety of benign and malignant conditions may derive from these varied elements (Table 1). An appropriate differential diagnosis may be formulated from a more comprehensive list by considering the specific imaging features of a given case (Table 2) (2,3). In this article, we discuss the differential diagnosis of space-occupying conditions in the presacral space and the imaging and demographic features necessary to narrow the possible diagnoses.

## Conditions with an Osteochondral Origin

### Giant Cell Tumor

Giant cell tumors are the most common sacral tumors after chordoma (4). Seven percent of giant cell tumors occur in the spine (5). Giant cell

**Table 2**
**Key Imaging Features of Presacral Masses**

| Type of Mass | Key Imaging Features |
|---|---|
| Osteochondral | |
| Giant cell tumor* | Lytic, expansile, often eccentrically located, vascular with substantial enhancement |
| Ewing sarcoma | Aggressive, permeative bone lysis, osseous expansion, sclerosis, soft-tissue mass |
| Osteosarcoma | Densely mineralized matrix, soft-tissue mass |
| Chondrosarcoma† | Chondroid matrix (rings and arcs), cartilaginous neoplasm, high water content (indicated by low attenuation at CT and high SI on T2W images) |
| Neurogenic | |
| Neurofibroma | Target appearance on T2W images (central area of low SI with a high-SI rim), low attenuation at CT |
| Schwannoma | Remodeling or erosion through sacral bone, heterogeneous mass with thin pseudocapsule and small cystic areas |
| Paraganglioma | Vascular tumor with intense enhancement and flow voids, hemorrhage common, cap sign related to hemorrhage (low-SI rim at MR imaging) |
| Chordoma‡ | Destructive lytic lesion, large presacral soft-tissue component, high SI on T2W images |
| Mesenchymal | |
| Hemangioma | Areas of fat and hemorrhage (increased SI on T1W images), increased SI on T2W with flow voids, phleboliths |
| Myelolipoma | Macroscopic fat, low attenuation at CT, high SI on T1W images that drops out with fat suppression |
| Solitary fibrous tumor | Well circumscribed, vascular with intense enhancement |
| Retroperitoneal fibrosis§ | Fibrotic plaque centered over lower lumbar spine, hypo- to isointense on T1W and T2W images, soft-tissue attenuation at CT |
| Gastrointestinal stromal tumor | Central areas of hemorrhage, necrosis, or cyst formation |
| Developmental cyst | Thin walled, uni- or multilocular, low attenuation at CT, high SI on T2W images, no internal enhancement |
| Germ cell tumor | Fat (low attenuation at CT and high SI on T1W images) |

Note.—SI = signal intensity, T1W = T1-weighted, T2W = T2-weighted.
*Giant cell tumors rarely metastasize to the lungs, and fluid-fluid levels have been reported. They may extend across the sacroiliac joints.
†The lungs are the most common site of metastasis.
‡Chordomas may extend across the sacroiliac joints.
§Retroperitoneal fibrosis may envelop the aorta, inferior vena cava, or ureters.

tumors tend to occur in the 2nd–4th decades of life and are more common in women than in men. Patients primarily present with pain (often radicular), weakness, and sensory deficits. Occasionally, a dramatic increase in size may be seen during pregnancy, a change presumably related to hormonal stimulation.

At imaging, as in other locations in the body, sacral giant cell tumors are seen as a locally aggressive, lytic, destructive, expansile lesion, often in an eccentric location (4). They commonly involve both sides of the midline and may extend across the sacroiliac joints (5). Five to ten percent of sacral giant cell tumors are malignant, with 1%–5% metastasizing to the lungs (4,6). Typically, computed tomography (CT) depicts a soft-tissue mass within the bone; the mass may have a thin sclerotic rim (4). Giant cell tumors are usually heterogeneous at magnetic resonance (MR) imaging, with intermediate signal intensity on T1- and T2-weighted images. There are case reports of fluid-fluid levels at MR imaging (7). Giant cell tumors are vascular neoplasms and demonstrate substantial enhancement at both CT and MR imaging, and they may contain areas of hemorrhage and necrosis (Fig 2).

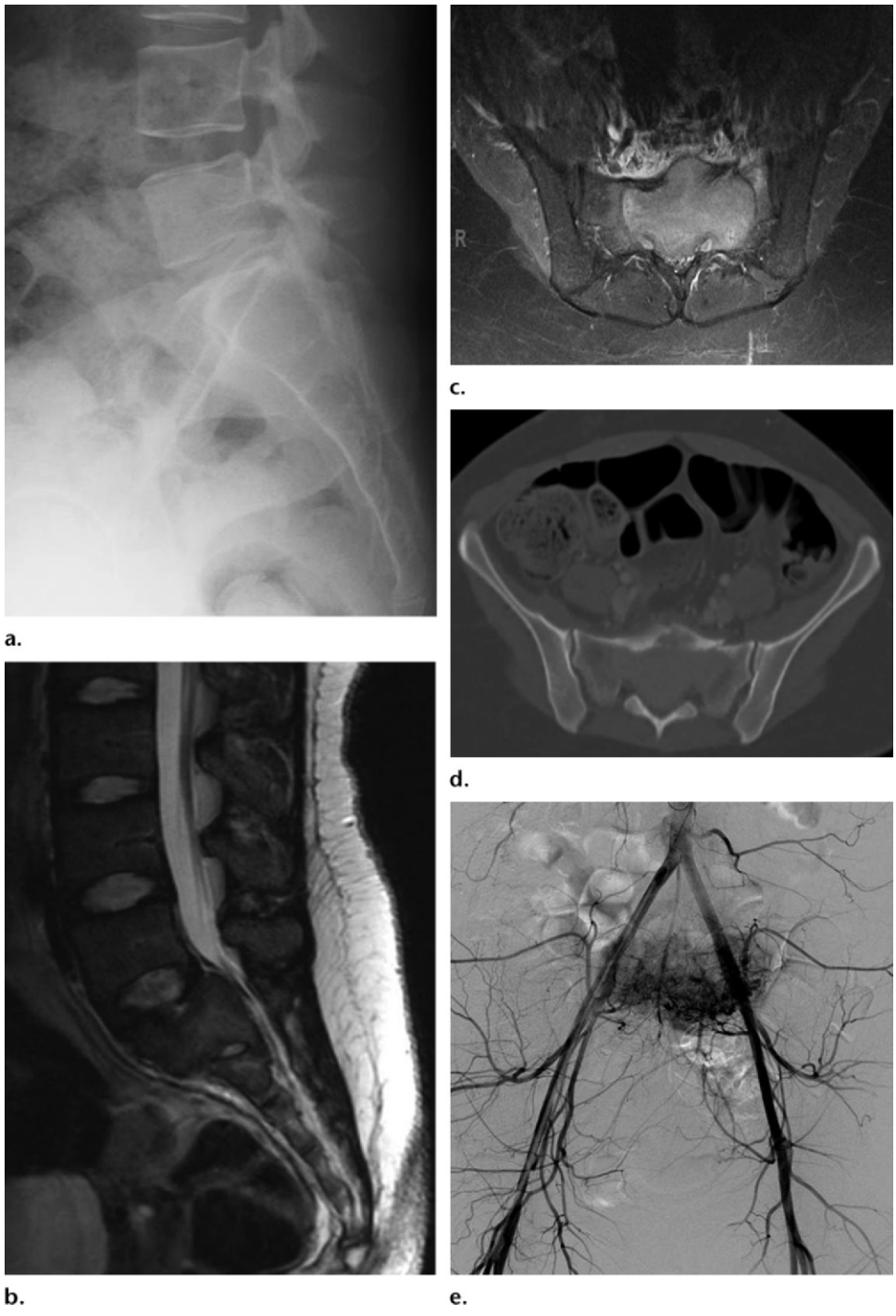


**Figure 2.** Giant cell tumor. **(a)** Lateral radiograph shows a lytic lesion involving S1 and S2. **(b)** Sagittal T2-weighted MR image shows that the lesion has heterogeneous signal intensity. **(c)** Axial contrast-enhanced T1-weighted MR image shows that the lesion demonstrates intense enhancement. **(d)** Axial CT image obtained with bone window settings clearly shows lytic bone destruction. **(e)** Angiogram shows that the lesion is hypervascular. A tumor blush is also seen.

In general, sacral lesions that spare most of the S1 segment and the sacroiliac joints are amenable to complete resection. If the size and location of the tumor preclude complete resection, treatment consists of a combination of partial curettage and radiation therapy (5). Recurrence rates of 40%–60% have been reported in cases of incomplete resection. Recurrent lesions manifest as a new area of bone destruction. Arterial embolization may also be performed before surgery, for palliation of symptoms, or in patients who are not eligible for surgery (6).

## Ewing Sarcoma

Three to ten percent of all primary Ewing sarcomas occur in the spine, but metastatic involvement is more common. Ewing sarcomas tend to occur in younger patients, with 90% of patients

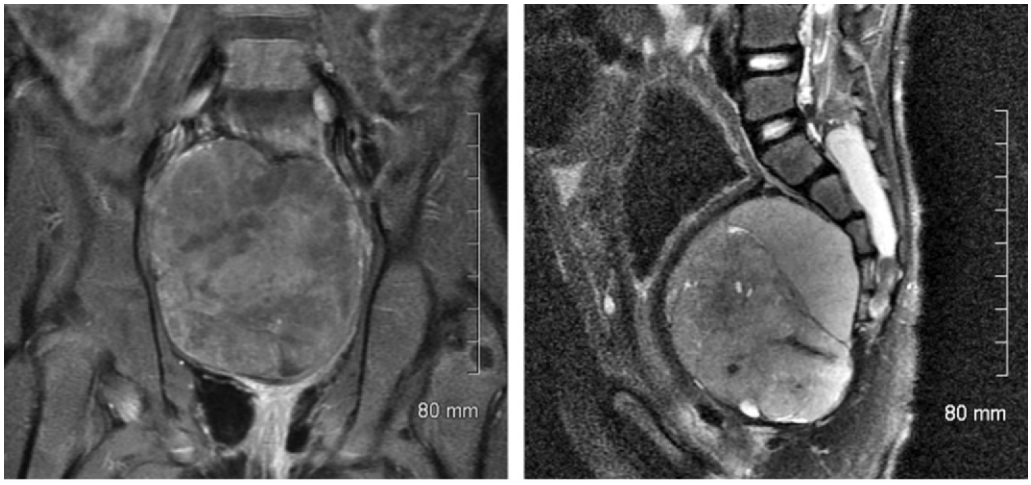


a. b.

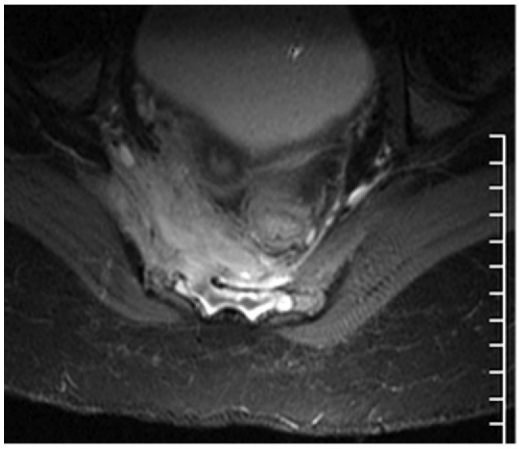

c.

**Figure 3.** Ewing sarcoma in two patients. **(a, b)** Coronal contrast-enhanced T1-weighted **(a)** and sagittal T2-weighted **(b)** MR images show a large heterogeneous presacral mass with intermediate to high signal intensity at T2-weighted imaging and heterogeneous enhancement. **(c)** Axial T2-weighted MR image in another patient shows an ill-defined high-signal-intensity presacral mass, associated bone involvement, and invasion of the sacrum.

presenting between the ages of 5 and 30 (4). At histologic analysis, Ewing sarcomas are composed of small, round, blue cells (5). At imaging, they are aggressive, demonstrating permeative bone lysis, osseous expansion, or sclerosis (5). Associated soft-tissue masses are common. The appearance of Ewing sarcoma at MR imaging is nonspecific, with intermediate signal intensity on T1-weighted images and intermediate to high signal intensity on T2-weighted images (Fig 3).

Radiation and chemotherapy are the standard treatments for patients with Ewing sarcoma, although those with neurologic instability or compromise may require surgical decompression and stabilization (5). Sacrococcygeal tumors are associated with a worse prognosis, most likely due to their delayed manifestation and large size. Sacrococcygeal tumors have a local control rate of approximately 63% and a long-term survival rate of 25% compared with nonsacral tumors, which have a local control rate of 100% and a long-term survival rate of 86%.

## Osteosarcoma

Osteosarcoma of the spine is rare, accounting for 0.6%–3.2% of all osteosarcomas and 5% of all primary malignant tumors of the spine (5). It may occur at all levels, but it has a predilection for the lumbosacral region. Patients with osteosarcoma of the spine are generally older, presenting, on average, in the 4th decade of life, and there is a male predominance. Most patients present with neurologic symptoms, and serum alkaline phosphatase levels may be elevated. At pathologic analysis, most spinal osteosarcomas are osteoblastic, although they may be chondroblastic or fibroblastic. Most spinal osteosarcomas are primary tumors, but they may occur secondary to radiation therapy or Paget disease.

Usually, radiography depicts a densely mineralized matrix, and CT and MR imaging are useful for evaluating the extent of involvement. Soft-tissue masses are common. Areas of dense matrix mineralization may have low signal intensity with all MR imaging sequences. Typically, osteosarcomas are large at the time of manifestation and preclude complete resection. Patients with osteosarcoma undergo adjuvant chemotherapy and radiation therapy, but their prognosis is poor, with death typically occurring within 1 year (5).

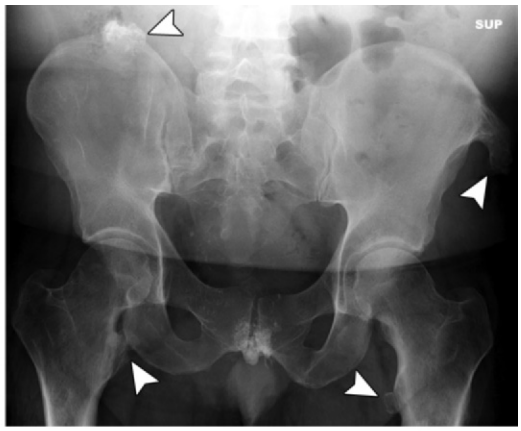


a.

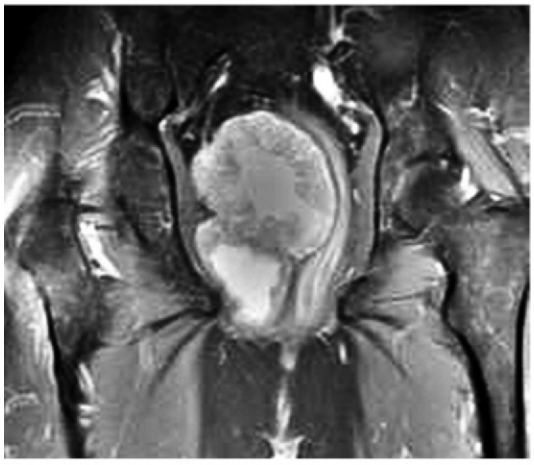

b.

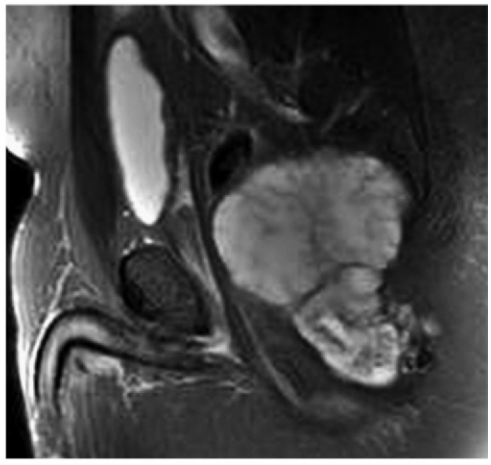

c.

**Figure 4.** Chondrosarcoma in a patient with multiple hereditary exostoses. **(a)** Axial radiograph of the pelvis shows multiple osteochondromas (arrowheads). An area of increased opacity is also seen in the lower sacrum, with areas of faint calcification. **(b, c)** Coronal T2-weighted **(b)** and sagittal contrast-enhanced T1-weighted **(c)** MR images show a large presacral mass with increased signal intensity at T2-weighted imaging and intense contrast enhancement.

## Chondrosarcoma

Three to twelve percent of primary chondrosarcomas occur in the spine, most commonly the thoracic spine (5). Chondrosarcomas manifest with pain and a palpable mass, and approximately 45% of patients have neurologic symptoms. The mean age at the time of presentation is 45 years, with a male predominance. Secondary malignant degeneration may occur in patients with a solitary osteochondroma or multiple hereditary exostoses.

Typically, bone destruction is seen at radiography, with the characteristic chondroid matrix (which appears as rings and arcs) seen in approximately 70% of cases. Cortical destruction and extension into the surrounding tissues are best depicted at CT and MR imaging. Usually, mineralization is present in the associated soft-tissue component. At CT, the attenuation of the nonmineralized portion is often lower than that of muscle due to the relatively high water content of hyaline cartilage. Nonmineralized areas have low to intermediate signal intensity on T1-weighted MR images and very high signal intensity on T2-weighted images, whereas areas of mineralization have low signal intensity with all pulse sequences (Fig 4).

Surgical resection is the standard treatment, with cure possible if the tumor is completely resected (5). Often, chondrosarcomas are low grade, and patients have a mean survival of 5.9 years. Radiation therapy may be used as an adjunct treatment, but its effectiveness is controversial. Chemotherapy is used to treat patients with a high-grade or dedifferentiated tumor. Although metastases are uncommon in patients with low-grade spinal chondrosarcomas, the most common site of metastasis is the lungs.

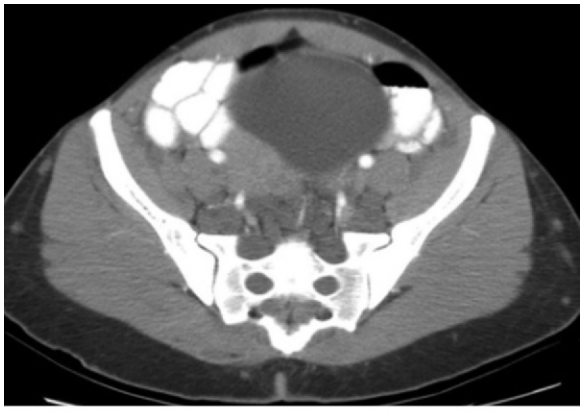

a.

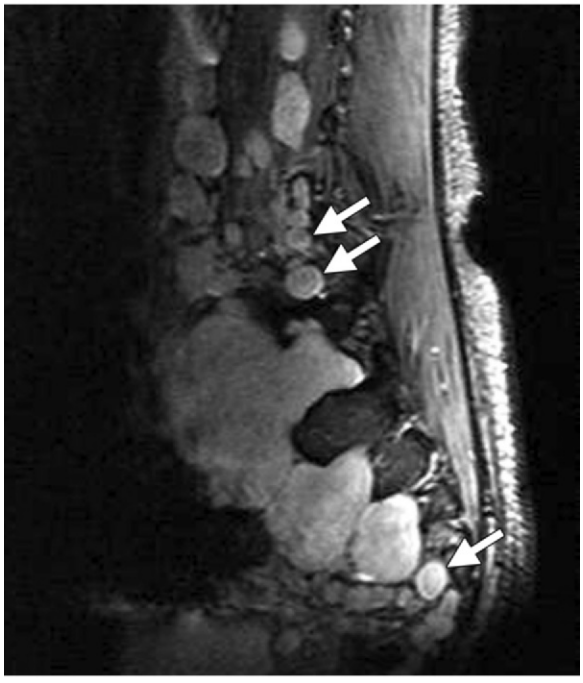

b.

**Figure 5.** Plexiform neurofibroma in two patients. **(a)** Axial CT image shows an area of low attenuation in the sacral plexus, a characteristic finding of plexiform neurofibroma. **(b)** Sagittal T2-weighted MR image obtained in another patient shows the target sign (arrows) in the sacral plexus, a finding characterized by an area of high signal intensity with a central area of low signal intensity that is suggestive of plexiform neurofibroma.

## Conditions with a Neurogenic Origin

### Neurofibromas

Neurofibromas are benign neural tumors that consist of fibroblasts, Schwann cells, and neural elements that expand and diffusely infiltrate a nerve (8). Neurofibromas most often occur in isolation, although multiple tumors may occur in patients with neurofibromatosis type 1 (NF1), an autosomal dominant condition that affects one in 2000–4000 people (3). A plexiform neurofibroma is characteristic of NF1 and fulfills one of the two criteria for diagnosing the condition. Such lesions may occur in the skin or subcutaneous tissues; craniofacial region; or paraspinal, mediastinal, visceral, or retroperitoneal region. Neurofibromas consist of an interdigitating, branching network of tumor located along a nerve and are typically bilateral and symmetric; asymmetric size or attenuation is concerning for malignant degeneration.

Typically, neurofibromas have low attenuation at CT, lower than that in adjacent soft tissues. They may resemble lymphadenopathy (3). They tend to be homogeneous at T1-weighted MR imaging, with isointense to mildly hyperintense signal intensity relative to that of muscle. At T2-weighted imaging, a target appearance that consists of a hyperintense rim of myxoid material and a central zone of low signal intensity related to their fibrous core is characteristic. Isolated neurofibromas may be difficult to distinguish from schwannomas, and neurofibromas may undergo malignant transformation (Fig 5) (4).

### Schwannomas

One to five percent of spinal schwannomas originate in the sacrum (3). Usually, they manifest as a large mass, and they may remodel or erode through the sacral bone, depending on their origin. At CT, schwannomas typically are seen as a heterogeneous presacral soft-tissue mass, with or without calcifications. They also tend to be heterogeneous at MR imaging, with low signal intensity on T1-weighted images and high signal intensity on T2-weighted images, and tend to have small cystic areas and a thin pseudocapsule (Fig 6).

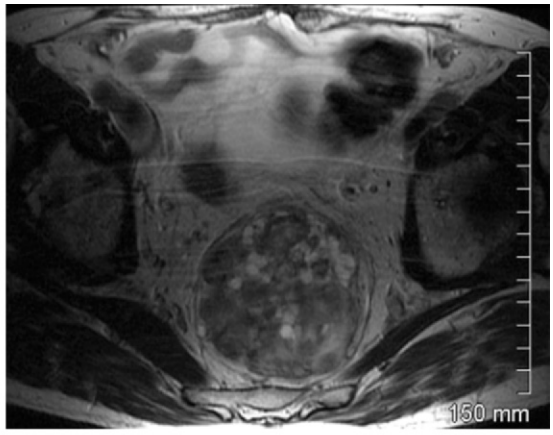


a.

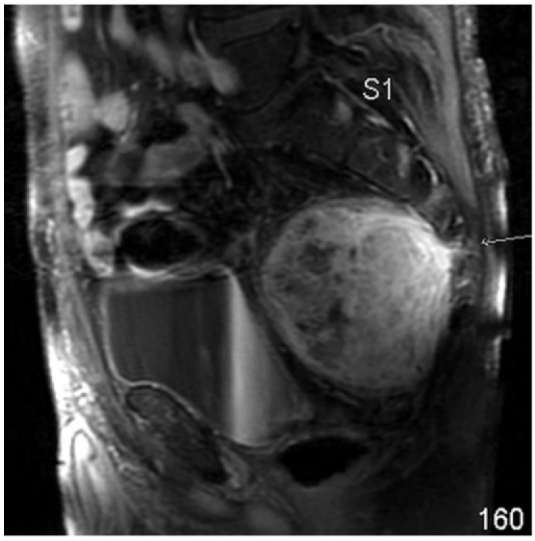


b.

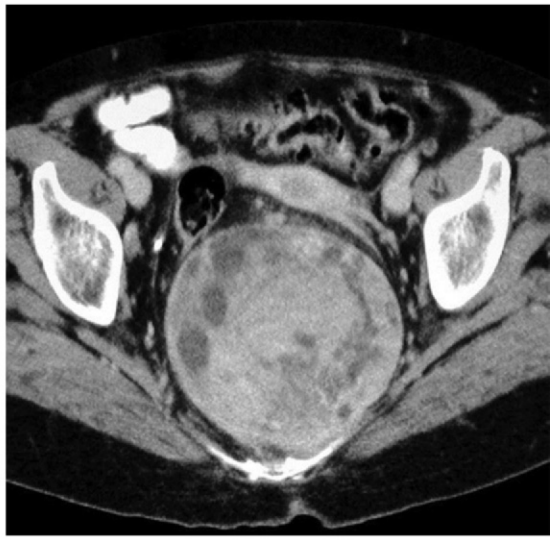

c.

**Figure 6.** Schwannoma in two patients. **(a)** Axial T2-weighted MR image shows a high-signal-intensity presacral mass with scattered cystic areas. **(b)** Sagittal contrast-enhanced T1-weighted MR image shows that the mass demonstrates heterogeneous enhancement. **(c)** Axial contrast-enhanced CT image in another patient shows a heterogeneously enhancing presacral mass.

## Perineural Cysts

Perineural cysts most commonly occur at the level of the second and third sacral nerve roots. The cyst wall is continuous with the arachnoid and dura, and the cyst cavity occupies the space between the perineurium and endoneurium (9). The cause of perineural cysts is uncertain; they may be congenital or traumatic. Stenosis of the ostium of the nerve root sheath allows cerebrospinal fluid (CSF) to flow in with arterial pulsation and restricts outflow. Perineural cysts may be symptomatic. In a study of 500 patients, approximately 5% had perineural cysts. Of those, 22% had a distribution of symptoms consistent with the cyst (9).

At CT, perineural cysts are seen as a cystic mass that is isoattenuating relative to CSF at the neural foramina (9). Bone remodeling and enlargement of the neural foramina may be seen, a result of increased CSF pressure. Because they communicate with CSF, perineural cysts fill with contrast material at CT myelography and have low signal intensity on T1-weighted MR images and high signal intensity on T2-weighted images. Treatment of perineural cysts includes surgical decompression and sacral laminectomy or percutaneous imaging-guided drainage (9). If the cyst must be completely removed, ganglia and nerve roots may need to be sacrificed.

## Dural Ectasia

Dural ectasia is present in 56%–65% of patients with Marfan syndrome (10). In dural ectasia, defective microfibrils weaken the dural sac, usually in the lumbosacral spine, where CSF pres-

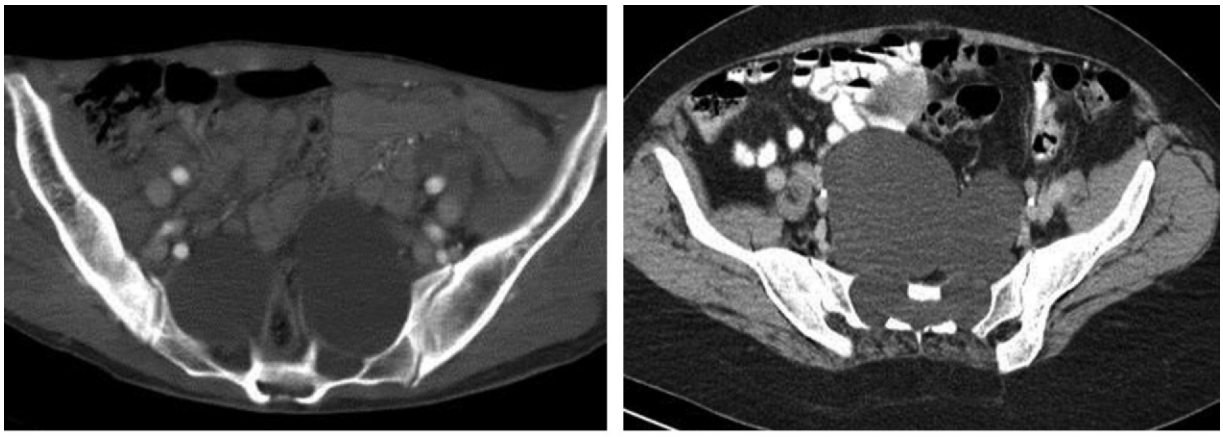

a. b.

**Figure 7.** Dural ectasia in a patient with Marfan syndrome. Axial contrast-enhanced CT images obtained with bone **(a)** and soft-tissue **(b)** window settings show dural ectasia with bone remodeling in the sacral foramina.

sure is greatest, which leads to incompetence. Typically, patients are asymptomatic, but they may present with back pain, headache, or neurologic deficits.

At imaging, dural ectasia may manifest with widening of the interpediculate distance and posterior vertebral body scalloping (10). MR imaging and CT best depict the extent of dural ectasia and any associated erosion of bone. Widening of the dural sac, dilatation of the nerve root sleeves, and scalloping of the posterior vertebral bodies may be seen in the lumbosacral spine (Fig 7).

## Anterior Myelomeningoceles

Anterior myelomeningoceles occur when the dural sac herniates through a defect in the anterior surface of the sacrum (11). The dural sac is composed of both the outer dura and the inner arachnoid membranes, and it contains CSF and, occasionally, neural elements. Anterior myelomeningoceles are most commonly congenital, and they are relatively rare, occurring in approximately one in 40,000 people (3). Eighty percent of anterior myelomeningoceles manifest in the 1st decade of life, and patients most commonly present with symptoms related to pressure on the pelvic organs and nerve roots, such as constipation, dysmenorrhea, and urinary incontinence. Back pain, numbness in the lower limbs, and headache are less common.

Osseous defects, such as vertebral body scalloping, hypoplasia, and aplasia, may accompany an anterior sacral meningocele and are best assessed at CT (3). However, MR imaging is preferred for overall assessment of meningoceles because it best depicts their neural elements and any associated sacral defects or dysraphism. Anterior myelomeningoceles may occur as part of the Currarino triad, which comprises an anorectal malformation, a sacrococcygeal osseous defect, and a presacral mass (3). The associated presacral mass may be a teratoma, anterior sacral meningocele, dermoid cyst, hamartoma, or enteric duplication cyst and is autosomal dominant in more than 50% of patients. Other associated congenital gastrointestinal and genitourinary anomalies include bicornuate uterus and duplicated vagina, duplicated kidney, renal pelvis or ureter, and anal atresia or stenosis (10). Generally, patients undergo surgical treatment because anterior sacral meningoceles do not spontaneously regress and the risk of complications increases with time (10). The mortality rate in patients who do not undergo surgery is 30%, a result of pelvic obstruction at the time of labor in childbearing women or erosion into the rectum, followed by meningitis in men and women of all ages.

Teaching Point

## Paragangliomas

Paragangliomas are neuroendocrine neoplasms that arise from the paraganglia, accessory organs of the peripheral nervous system (12). They most commonly occur in the adrenal glands (where they are called pheochromocytomas), carotid body (where they are called carotid body tumors), jugular foramen (where they are called

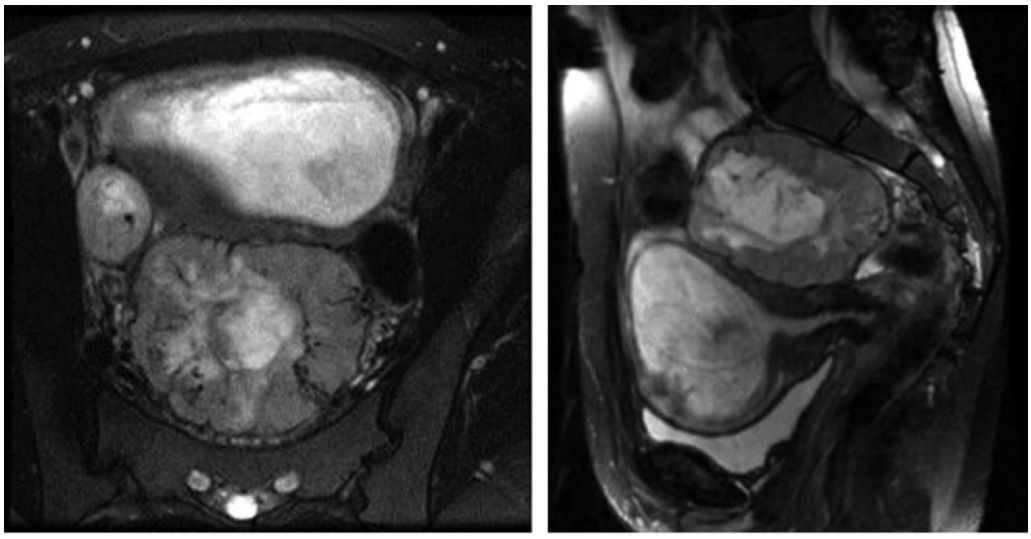

a. b.

**Figure 8.** Paraganglioma in a pregnant woman. Axial **(a)** and sagittal **(b)** T2-weighted MR images show a large presacral mass that is iso- to hyperintense with a hypointense rim, a finding known as the cap sign.

glomus jugulare tumors), and near the vagus nerve (where they are called vagal paragangliomas). They are less common at other sites, such as the filum terminale. Typically, spinal paragangliomas are intradural, extramedullary lesions located in the region of the cauda equina and filum terminale (12). In general, patients present with long-term low back pain and sciatica that last, on average, 4 years until a diagnosis of paraganglioma is made. Paragangliomas are slightly more common in men, and the average age at presentation is 46 years.

Paragangliomas are highly vascular tumors that demonstrate an intense, early blush at angiography that persists into the late arterial and early venous phases (12). Typically, they are seen as a well-circumscribed mass that is isointense on T1-weighted MR images and iso- to hyperintense on T2-weighted MR images. Hemorrhage is common, and a low-signal-intensity rim (the cap sign) may be seen. Intense enhancement is seen on contrast-enhanced images, and flow voids are common (Fig 8).

Teaching Point

## Chordomas

Chordomas arise from notochordal rests and are limited to the clivus, spine, and sacrum on the basis of their cell of origin (4,5). They are the most common primary sacral tumor (4). Approximately 50% of chordomas occur in the sacrum and coccyx; 35% occur in the clivus; and 15% occur in the spine, most commonly the cervical and lumbar regions. They are typically located in the midline or paramedian region and account for 2%–4% of all malignant bone neoplasms.

Chordomas are most common in the 4th–7th decades of life, but they may occur in all age groups (4). Spinal chordomas are twice as common in men as they are in women. Because chordomas are slow-growing, patients typically have nonspecific symptoms, including low back and sacral pain, retention of urine, and radicular pain (13). Given this subtle manifestation, patients commonly present with a large, bulky mass.

Chordomas are destructive lytic lesions that may extend across the sacroiliac joints (4). Calcification is common in sacrococcygeal lesions and is seen on 50%–70% of radiographs and 90% of CT images (5). Usually, a large presacral soft-tissue component is present, with soft tissues extending into the sacral canal. Chordomas have low to intermediate signal intensity on T1-weighted MR images and high signal intensity on T2-weighted MR images, with variable, often only moderate, contrast enhancement (Fig 9).

Treatment of chordomas consists of surgical resection and radiation therapy (5). Chordomas are locally aggressive neoplasms, and complete resection may be difficult in locations such as the clivus and sacrum. The prognosis is better

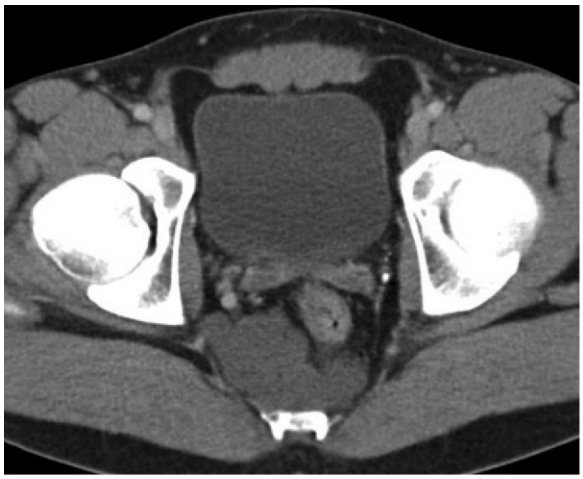

a.

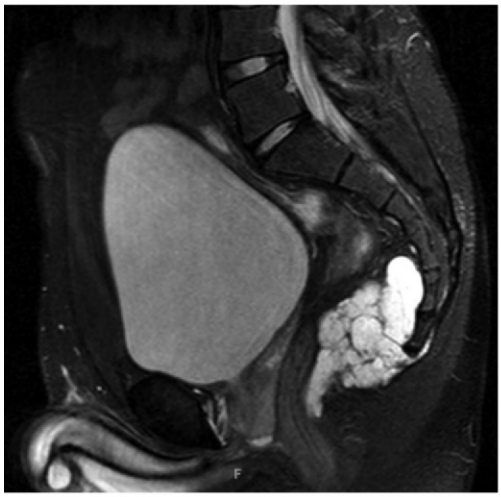

b.

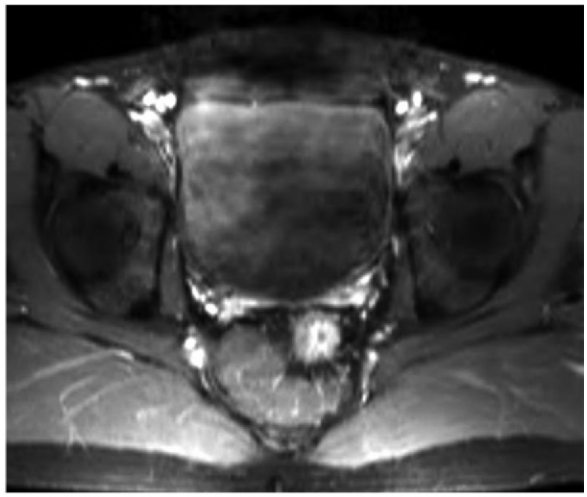

c.

**Figure 9.** Chordoma. **(a)** Axial contrast-enhanced CT image shows a homogeneous mass anterior to the distal sacrum and coccyx. **(b)** Sagittal T2-weighted MR image shows the hyperintense mass. **(c)** Axial contrast-enhanced T1-weighted MR image shows that the mass demonstrates only mild enhancement.

for patients with a sacrococcygeal lesion, with an average survival of 8–10 years compared with 4–5 years for those with a chordoma in another location. Local recurrence is the most important predictor of mortality and is usually related to the extent of the initial resection (14). Metastases are present in 5%–43% of patients, most commonly in the liver, lungs, regional lymph nodes, peritoneum, skin, and heart.

## Conditions with a Mesenchymal Origin

### Hemangiomas

Hemangiomas are the most common soft-tissue abnormality, accounting for approximately 7% of all benign soft-tissue tumors (15). In addition, they are the most common tumors in infants and usually appear within the 1st week of life (16). Neonates with a hemangioma undergo a postnatal period of rapid proliferation from 3 to 9 months of age, followed by a period of variable stability and slow involution. Hemangiomas are three times more common in girls than in boys, and the neck is the most common location, followed by the trunk (25%) and extremities (15%). Most hemangiomas are seen at clinical examination and do not require further investigation or treatment because they will spontaneously resolve. Imaging is performed in patients with a deep hemangioma and normal overlying skin or an atypical soft-tissue mass; to evaluate extension of a mass; and to evaluate a lesion that compromises the airway, impairs vision, causes heart failure, or induces thrombocytopenic coagulopathy. Imaging may also be used to help guide therapy.

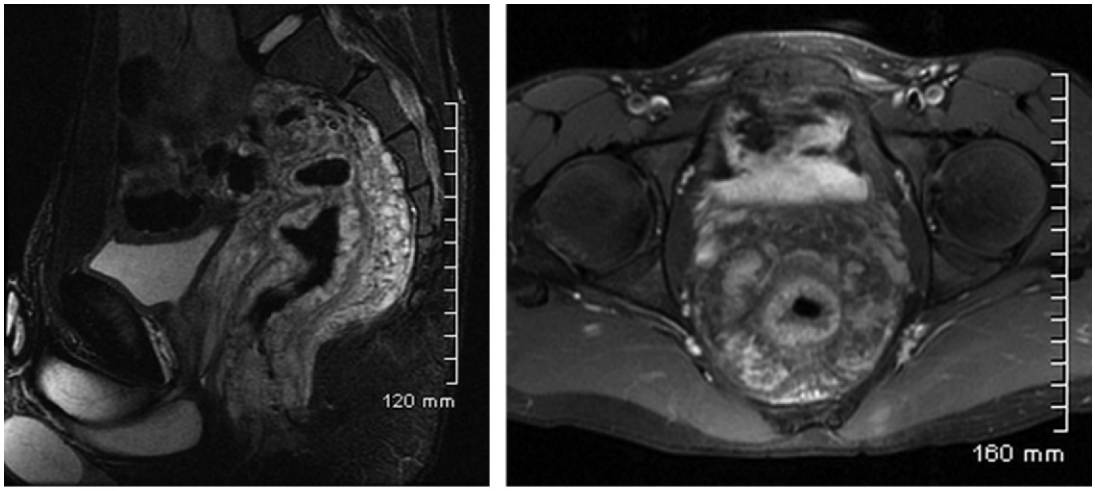


a. b. c.

**Figure 10.** Perirectal hemangioma in two patients. **(a)** Sagittal short inversion time inversion-recovery MR image shows a perirectal mass with heterogeneous high signal intensity. **(b)** Axial contrast-enhanced T1-weighted MR image shows that the mass demonstrates heterogeneous enhancement. **(c)** Axial contrast-enhanced CT image obtained in another patient shows phleboliths, a typical finding of perirectal hemangioma.

Typically, hemangiomas are superficial, but they may involve deeper structures, such as the skeletal muscles (15). They have intermediate signal intensity on T1-weighted MR images and high signal intensity and flow voids on T2-weighted images (Fig 10) (16). On T2-weighted images, clusters of high-signal-intensity lobules indicate cystic vascular spaces that contain stagnant blood (15). Areas of increased signal intensity on T1- and T2-weighted images correlate with hemorrhage and areas of fat deposition. Phleboliths are common and appear as low-signal-intensity foci on both T1- and T2-weighted images.

## Myelolipoma

Myelolipomas are benign tumors composed of mature fat and scattered hematopoietic cells (17). They most commonly occur in the adrenal gland. Extra-adrenal myelolipomas most commonly occur in the retroperitoneum, but they may also be found in the chest or pelvis. At CT, they typically appear as a hypovascular mass that contains macroscopic fat with areas of soft-tissue attenuation interspersed (Fig 11). The amount of fat within a myelolipoma varies. At T1-weighted MR imaging, the fatty areas have high signal intensity that drops out when fat is suppressed. Persistent high signal intensity is usually related to hemorrhage or marrow elements.

Teaching Point

## Solitary Fibrous Tumors

Solitary fibrous tumors are mesenchymal tumors of fibroblastic or myofibroblastic origin. Hemangiopericytomas and solitary fibrous tumors are part of a spectrum and have overlapping histologic features, which caused many solitary fibrous tumors to be incorrectly classified as hemangio-

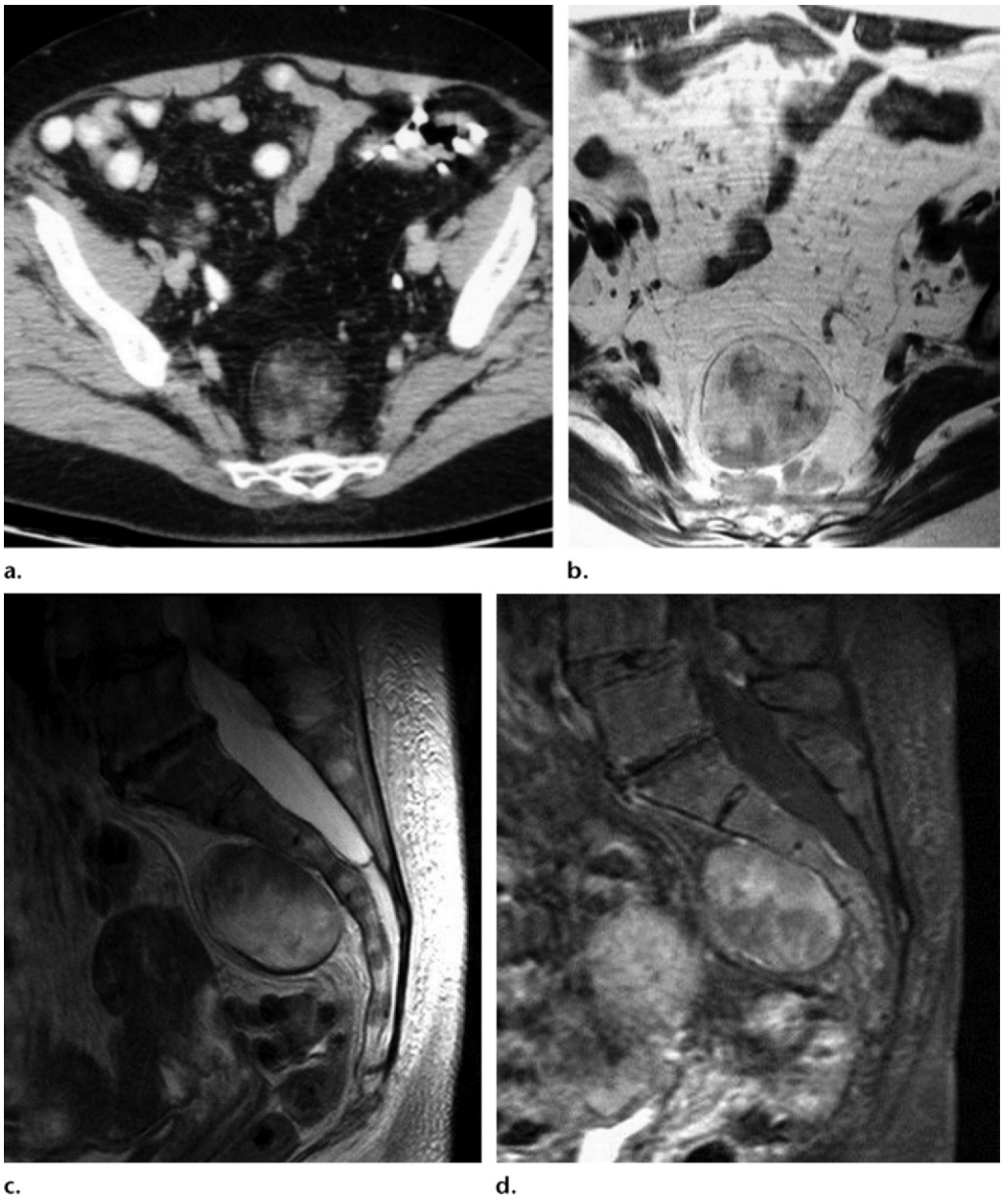


**Figure 11.** Myelolipoma. **(a)** Axial contrast-enhanced CT image shows a well-circumscribed presacral mass with macroscopic fat. **(b, c)** Axial **(b)** and sagittal **(c)** T1-weighted MR images show that the areas of fat demonstrate increased signal intensity. **(d)** Sagittal T1-weighted fat-suppressed MR image shows dropout of signal intensity in the areas of fat.

Teaching Point

pericytomas in the past. Solitary fibrous tumors may occur anywhere in the body. It was recently established that extrapleural tumors are more common than pleural tumors (18).

Typically, solitary fibrous tumors manifest as a slow-growing mass in middle-aged adults (18). Symptoms are uncommon, but, when present, they may be related to local mass effect. CT depicts a well-circumscribed mass with soft-tissue attenuation that typically demonstrates intense contrast enhancement (Fig 12) (18,19). Areas of hemorrhage, necrosis, and cystic change may be seen. Typically, solitary fibrous tumors have low to intermediate signal intensity on T1- and T2-weighted MR images, a result of fibrous tissue,

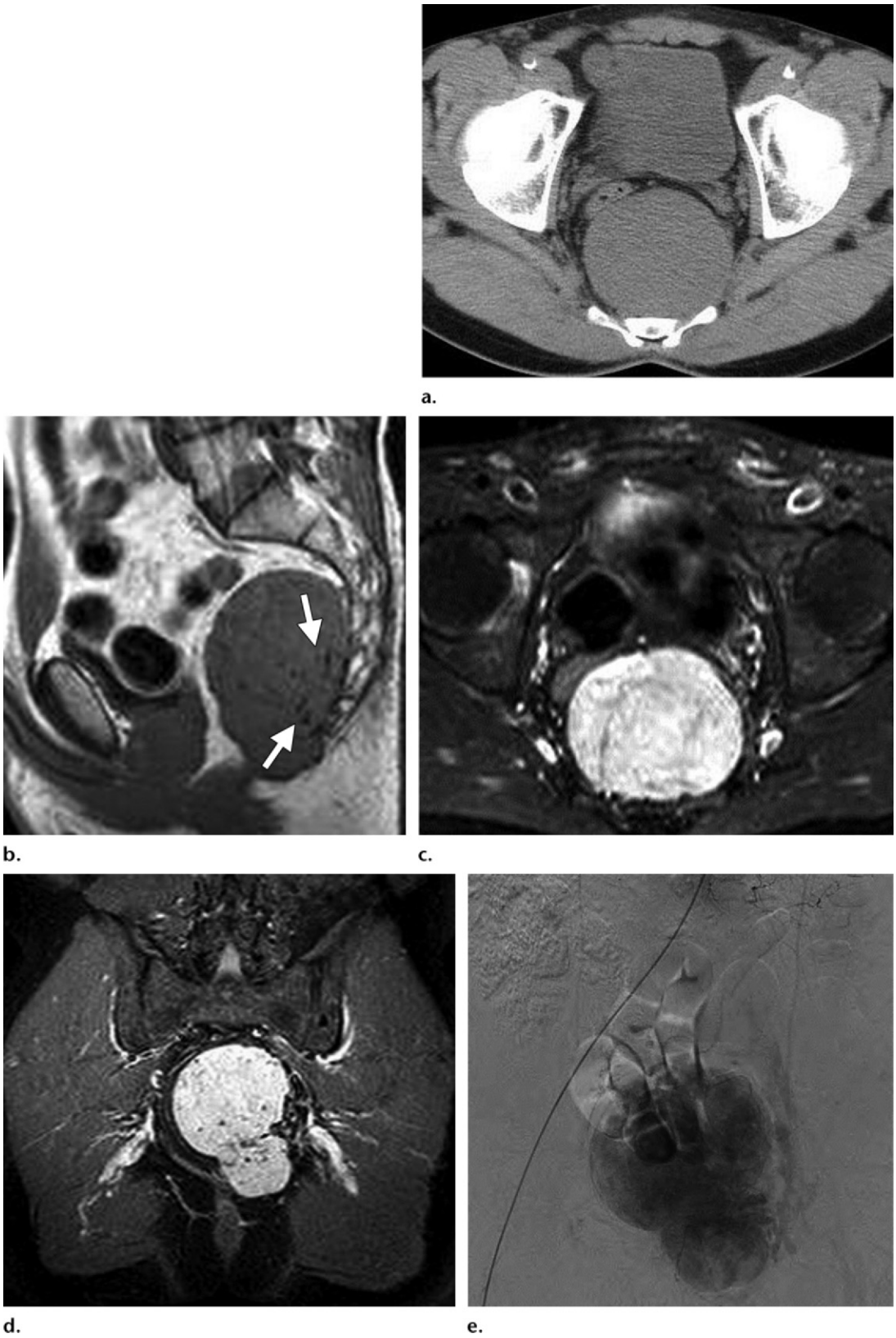


**Figure 12.** Solitary fibrous tumor. **(a)** Axial contrast-enhanced CT image shows a homogeneous mass that is isoattenuating relative to muscle. **(b)** Sagittal T1-weighted MR image shows flow voids (arrows) in the low-signal-intensity mass. **(c, d)** Axial **(c)** and coronal **(d)** contrast-enhanced T1-weighted MR images show that the mass demonstrates intense enhancement. **(e)** Angiogram shows the tumor, which demonstrates increased vascularity.

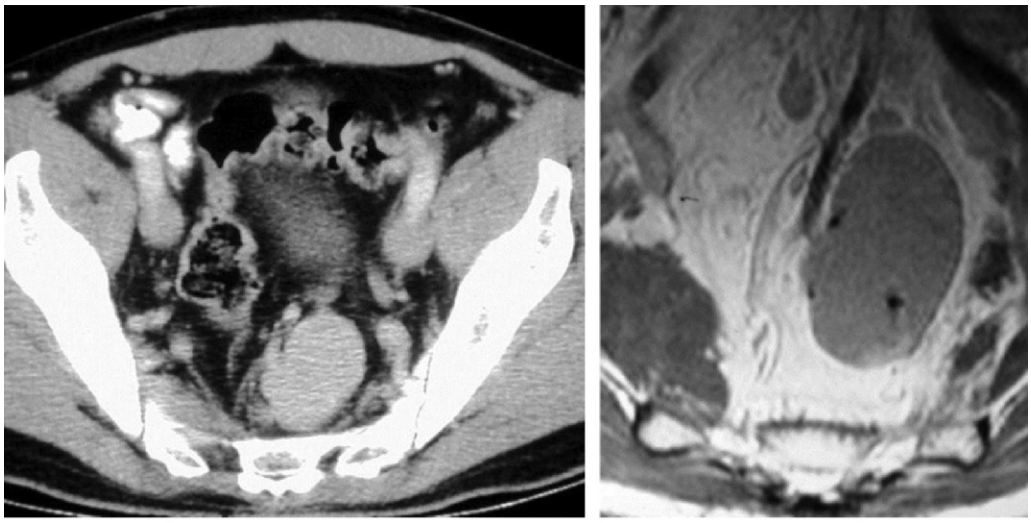

a. b.

**Figure 13.** Castleman disease. **(a)** Axial contrast-enhanced CT image shows a well-circumscribed mass with intense contrast enhancement. **(b)** Axial T1-weighted MR image shows that the mass is mildly hyperintense relative to muscle, with several flow voids.

but areas of myxoid or cystic degeneration may demonstrate high signal intensity on T2-weighted images. Hypervascularity with prominent enhancement and flow voids is common.

## Castleman Disease

Castleman disease is a disorder of nonclonal lymph node hyperplasia that most commonly occurs in the chest (20). It primarily involves lymphatic tissues, but extralymphatic sites, such as the lungs, larynx, parotid glands, pancreas, meninges, and muscles, may be involved. The hyaline vascular form of the disease is the most common, is typically diagnosed in the 3rd or 4th decade of life, tends to be unicentric, and manifests with an asymptomatic mass (20,21).

At imaging, Castleman disease typically appears as a single enlarged lymph node or a conglomerate nodal mass with intense, homogeneous contrast enhancement (20,21). Internal calcifications may be seen in as many as 10% of lesions. At MR imaging, lesions tend to be heterogeneously hyperintense relative to skeletal muscle on both T1- and T2-weighted images. Flow voids may be present (Fig 13).

## Retroperitoneal Fibrosis

Retroperitoneal fibrosis is relatively rare, with a prevalence of 1 in 200,000 people (22). Most cases are idiopathic but may be related to antigens from atheromatous plaque. Other causes include medications, retroperitoneal hemorrhage or extravasation of urine, and a desmoplastic response to tumors. As many as 15% of patients have an additional fibrotic process located outside the retroperitoneum, such as mediastinal fibrosis, Riedel fibrosing thyroiditis, sclerosing cholangitis, and fibrotic orbital pseudotumors. Symptoms of retroperitoneal fibrosis are related to entrapment and compression, most commonly of the ureters, leading to costovertebral angle pain, ureteral colic, oliguria, anuria, and eventually renal failure. Entrapment of the inferior vena cava may lead to lower extremity edema and deep thrombophlebitis, involvement of the gonadal veins may lead to hydrocele and scrotal discomfort, and arterial entrapment may lead to lower extremity claudication and gangrene, renovascular hypertension, and bowel ischemia, depending on the vessels involved.

Retroperitoneal fibrosis most commonly manifests as an isolated fibrotic plaque centered over the lower lumbar spine (22). Typically, the plaque begins below the aortic bifurcation and spreads superiorly along the anterior surface of the spine, enveloping the aorta, inferior vena cava, and, often, the ureters in the margins. At CT, the plaque may be midline or asymmetric and may be well-circumscribed or poorly defined. It demonstrates soft-tissue attenuation and variable contrast enhancement, with immature plaque demonstrating greater enhancement. It is hypo- to isointense on both T1- and T2-weighted MR images; an area of hyperintensity is concerning for inflammatory edema or an associated malignancy (Fig 14).

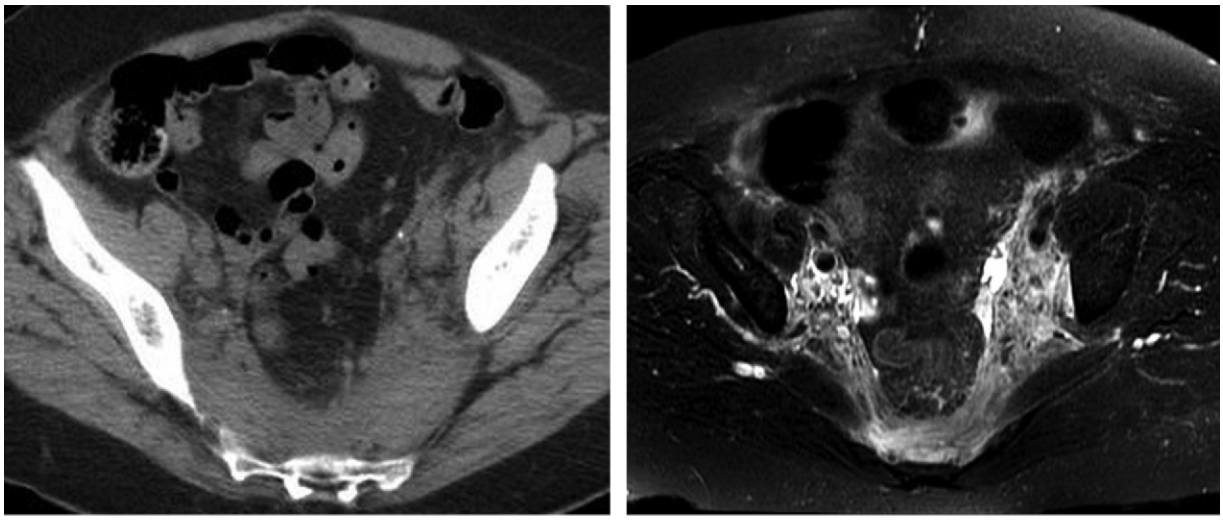

a. b.

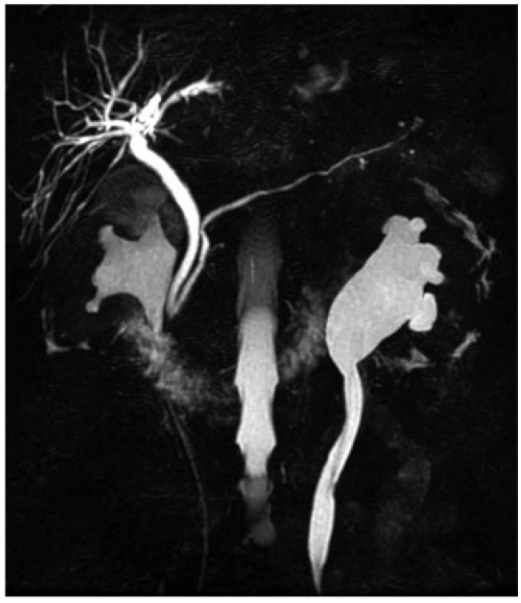

c.

**Figure 14.** Retroperitoneal fibrosis. **(a)** Axial contrast-enhanced CT image shows an ill-defined presacral mass. **(b)** Axial contrast-enhanced T1-weighted MR image shows that the mass demonstrates enhancement. **(c)** T2-weighted MR cholangiopancreatographic image shows bilateral hydronephrosis, a result of fibrosis surrounding the distal ureters.

Treatment of retroperitoneal fibrosis consists of ceasing any inciting medications and initiating corticosteroid therapy (22). In early idiopathic disease, improvement and relief of ureteral obstruction typically occur within 7–10 days. Patients with more resistant fibrosis may undergo azathioprine therapy. Ureterolysis, indwelling ureteral stents, and percutaneous nephrostomy are used to treat associated ureteral obstruction. Patients with idiopathic retroperitoneal fibrosis and no significant renal compromise have an excellent prognosis, with long term success reported in more than 90% of patients.

## Lymphomas

Lymphomas are soft tumors that tend to grow around and displace structures such as blood vessels and the bowel. They may lead to lymphadenopathy almost anywhere in the body (23). Lymphomas most often involve the chest, retroperitoneum, or superficial lymph node chains; as the disease progresses, lymph nodes often coalesce, forming conglomerate masses. At CT, lymphomas have soft-tissue attenuation with homogeneous enhancement (Fig 15) (23). Occasionally, peripheral enhancement may be seen. At MR imaging, they are characterized by an area of low signal intensity on T1-weighted images and an area of high signal intensity on T2-weighted images. Treatment of lymphomas consists of a combination of chemo- and radiation therapy, depending on the stage and grade of the tumor.

## Gastrointestinal Stromal Tumors

Gastrointestinal stromal tumors are the most common mesenchymal neoplasms in the gastrointestinal tract (24). Their best defining feature is expression of KIT (CD117), a tyrosine kinase factor receptor. Gastrointestinal stromal tumors most commonly occur in older patients and have a slight male predominance, with an increased prevalence in patients with NF1. Their clinical manifestation depends on the location in the body; they are most common in the stomach (70%) and small intestine (20%–30%). Colonic and esophageal tumors most commonly manifest with bleeding, a result of mucosal ulceration.

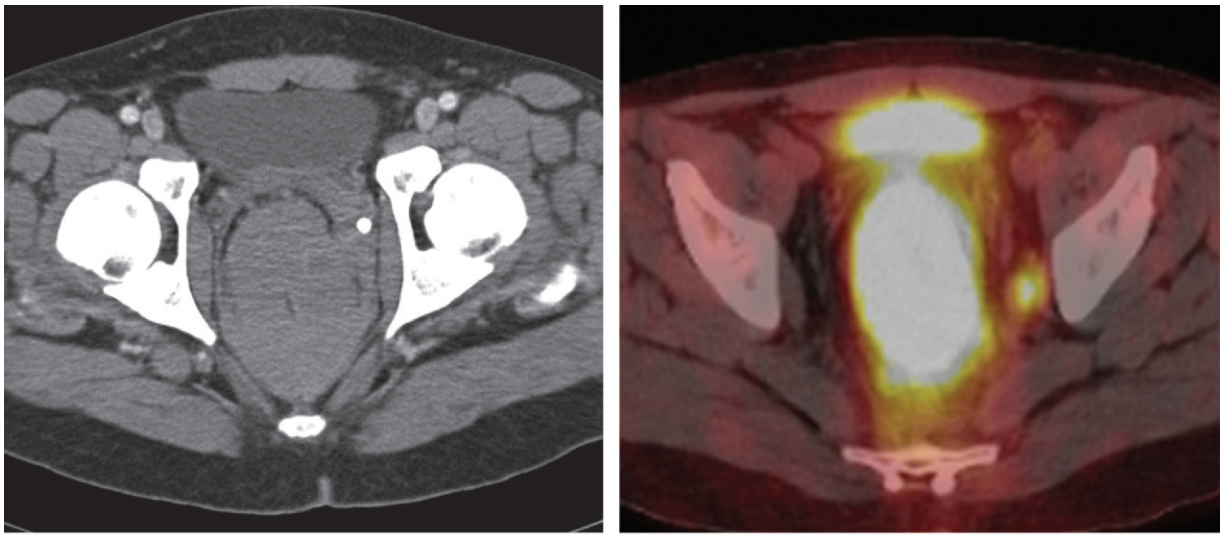

a. b.

**Figure 15.** Non-Hodgkin–type B-cell lymphoma. **(a)** Axial contrast-enhanced CT image shows an abnormal area of homogeneous enhancement in the rectal and perirectal soft tissues. **(b)** Positron emission tomographic (PET)/CT image shows an area of intense uptake that corresponds to the abnormal rectal and perirectal soft tissues seen at CT.

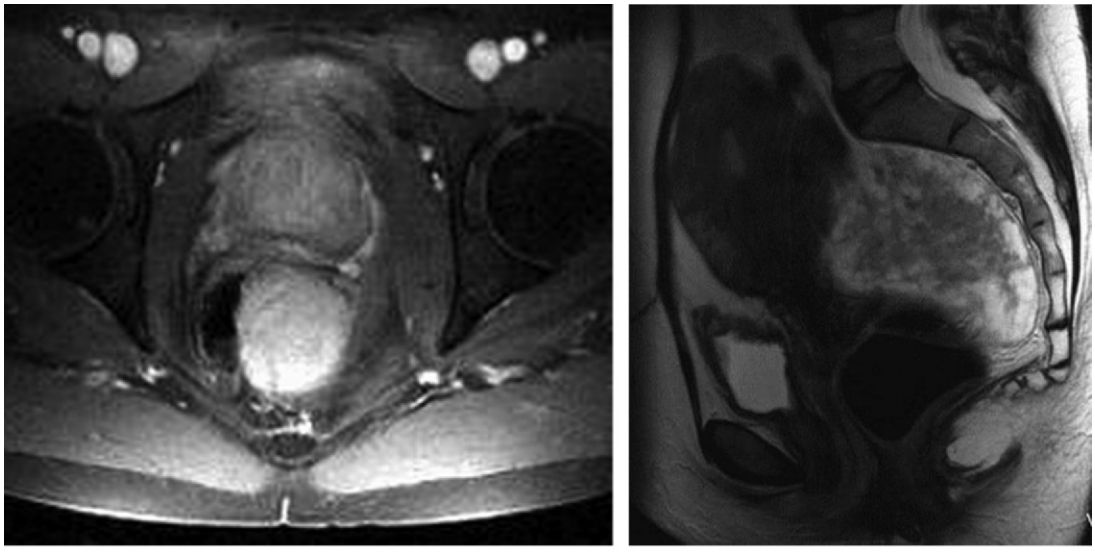

a. b.

**Figure 16.** Gastrointestinal stromal tumor in two patients. **(a)** Axial contrast-enhanced T1-weighted MR image shows a perirectal presacral mass that demonstrates intense enhancement. **(b)** Sagittal T2-weighted MR image in another patient shows a larger mass with heterogeneous signal intensity.

Patients with a gastrointestinal stromal tumor present with hematemesis; melena; hematochezia; or anemia, which is caused by occult bleeding. Those with a tumor in the stomach or small intestine may present with nausea, vomiting, abdominal pain, weight loss, abdominal distention, or intestinal obstruction.

Gastrointestinal stromal tumors usually involve the outer muscular layer and tend to be exophytic. When located in the anorectal region, they tend to expand to the rectal wall, resulting in a focal well-circumscribed mural mass (24). At CT, they have soft-tissue attenuation with a central area of low attenuation resulting from hemorrhage, necrosis, or cyst formation. Peripheral enhancement is common. Typically, an area of uniform intermediate signal intensity is seen on T1-weighted MR images and an area of heterogeneous high signal intensity is seen on T2-weighted images, with heterogeneous enhancement (Fig 16). Extension into the ischiorectal fossa, prostate, or vagina may be present.

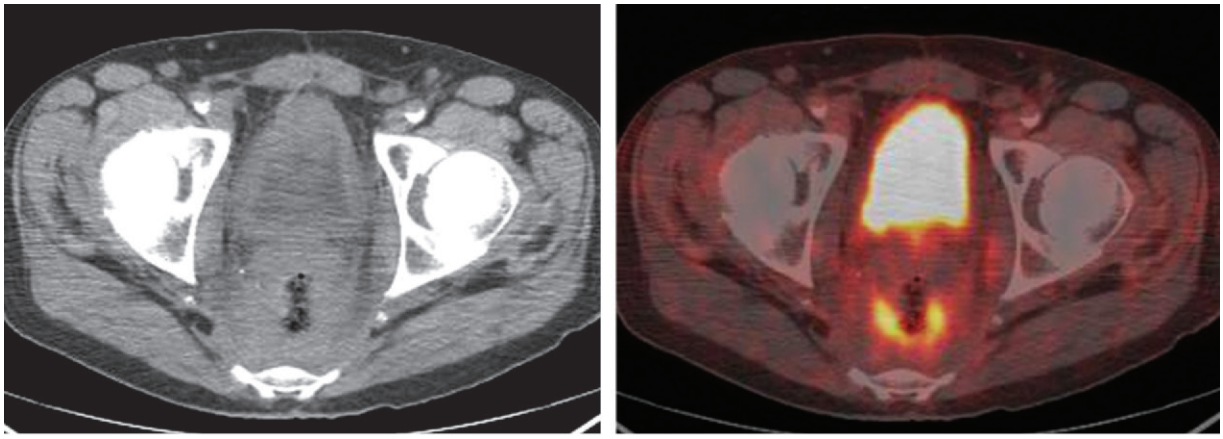

a. b.

**Figure 17.** Recurrent rectal adenocarcinoma. **(a)** Axial contrast-enhanced CT image shows abnormal perirectal and presacral soft tissues. **(b)** Axial PET/CT image shows intense uptake in the perirectal and presacral soft tissues, a finding consistent with recurrence.

Treatment of gastrointestinal stromal tumors depends on the size of the tumor and its mitotic rate (24). A small number of tumors recur or metastasize, even when they appear to be histologically benign. Patients with a recurrent tumor have a poor prognosis. Conventional therapy consists of surgical resection. Imatinib (Gleevec; Novartis, East Hanover, NJ), a chemotherapeutic agent, is used to target tyrosine kinase; 59%–69% of patients respond to imatinib therapy. Malignant tumors tend to recur and metastasize to the liver and peritoneal surfaces. Systemic and intraperitoneal chemotherapy, arterial chemoembolization, surgery, and radiation therapy tend to be ineffective for treating recurrent and metastatic disease.

## Metastatic Disease

Approximately 40,000 cases of rectal cancer are diagnosed each year (25). The lifetime risk for developing a colorectal malignancy is 5.9%, and one-third of cases occur in the rectum. The peak prevalence of rectal adenocarcinoma is in the 7th decade of life, and patients tend to present with gastrointestinal bleeding or a change in bowel movement habits. At imaging, rectal adenocarcinomas appear as a polypoid mass that increases in size and eventually infiltrates the bowel wall. In patients with a primary tumor that extends beyond the rectal wall (T3 or T4), they may manifest as a presacral mass or be seen as a local recurrence. Posttreatment changes resulting from chemoradiation therapy may lead to abnormal presacral soft tissue, making evaluation for recurrent tumor difficult. In this setting, PET may be useful to identify recurrent tumor (Fig 17). Metser et al (26) reported that PET/CT had sensitivity of 97.3% for depicting recurrent rectal adenocarcinoma, whereas contrast material–enhanced CT had sensitivity of 70.3%. Among the lesions that were missed at CT and depicted at PET/CT, five were a local recurrence in the presacral space. Other epithelial malignancies may also give rise to metastatic disease in the presacral space.

## Conditions with an Unknown Origin

Desmoplastic small round-cell tumors are a rare malignancy, with an unknown origin (27,28). Histologically, they belong to the family of primitive pediatric tumors composed of small, round, blue cells, including Wilms tumor, Ewing sarcoma, peripheral primitive neuroectodermal tumor, and Askin tumor. Typically, desmoplastic small round-cell tumors occur in adolescent boys and young men. They are usually large and bulky at presentation and tend to diffusely spread throughout the peritoneal surfaces. A solitary peritoneal mass may be the only finding at initial manifestation, with peritoneal thickening,

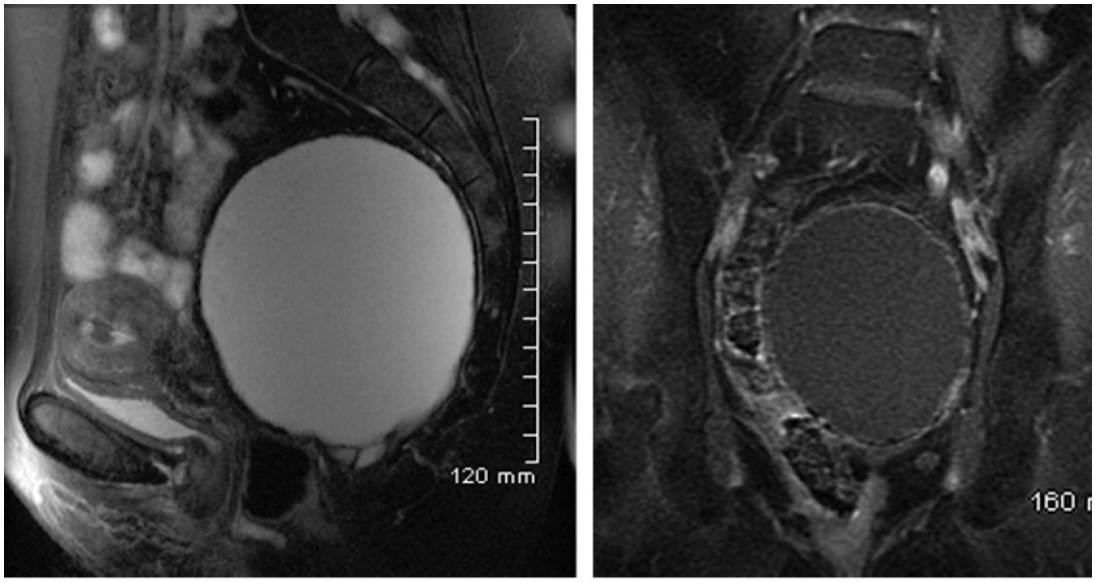


a. b.

**Figure 18.** Rectal duplication cyst. **(a)** Sagittal T2-weighted MR image shows a large hyperintense presacral cystic mass. **(b)** Coronal contrast-enhanced T1-weighted MR image shows a thin area of peripheral enhancement around the mass.

nodules, and masses seen in patients with more advanced disease.

At CT, desmoplastic small round-cell tumors tend to be heterogeneous with a central area of low attenuation, a result of hemorrhage and necrosis (28). They may contain punctate calcifications, and malignant ascites is often present. They have heterogeneous signal intensity at MR imaging, with predominantly hypointense signal intensity on T1-weighted images and hyperintense signal intensity on T2-weighted images. They demonstrate heterogeneous enhancement after administration of contrast material. Metastases are present in 50% of patients at presentation, most commonly to the liver, lungs, and bones. Patients with desmoplastic small round-cell tumors have a universally poor prognosis (3-year survival rate of <30%), even with treatment.

## Congenital and Developmental Conditions

### Developmental Cysts

Developmental cysts are the most common congenital condition in the presacral space and include epidermoid, dermoid, enteric, tailgut (also known as retrorectal cystic hamartoma), and duplication cysts (29). Developmental cysts typically manifest during childhood, and they are relatively rare in adults. However, tailgut cysts are the most common asymptomatic presacral lesions that are incidentally found in adults (30). Among patients with an incidentally discovered lesion, 50% are asymptomatic. When present, symptoms are related to mass effect from local compression on the rectum and lower urinary tract and lead to constipation, rectal fullness, painful defecation, lower abdominal pain, dysuria, and urinary frequency. The most important complications of developmental cysts are infection and fistula formation; 30%–50% of developmental cysts are complicated by chronic infection. Bleeding related to ectopic gastric mucosa or mucosal irritation is rare, as is malignant degeneration.

Teaching Point

Developmental cysts tend to be thin-walled and may be uni- or multilocular (Figs 18, 19) (29). Internal echoes related to mucoid material or inflammatory debris may be seen at ultrasonography (US). They have low attenuation at CT, with no associated enhancement, and associated thin calcifications are rare. If they are secondarily

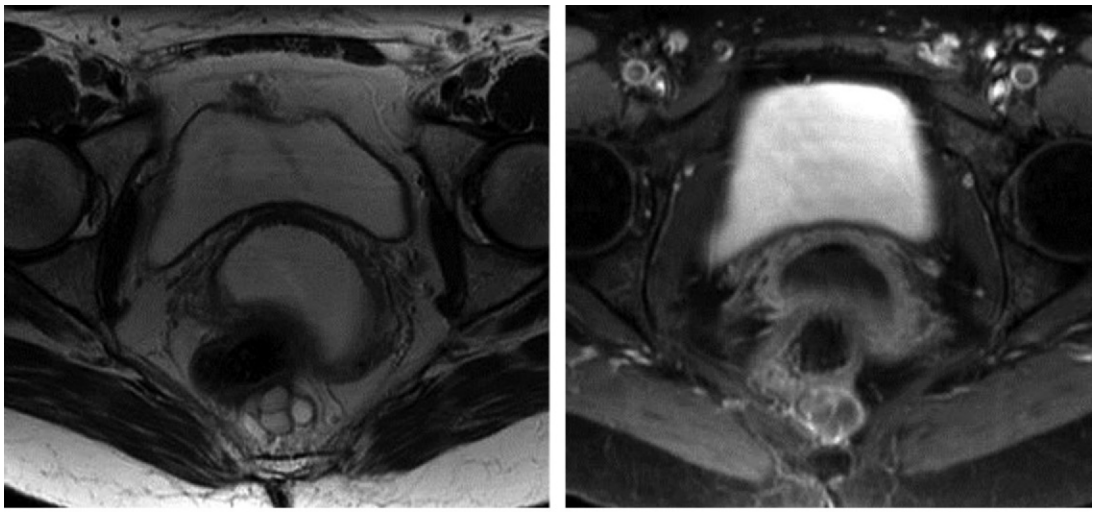

a. b.

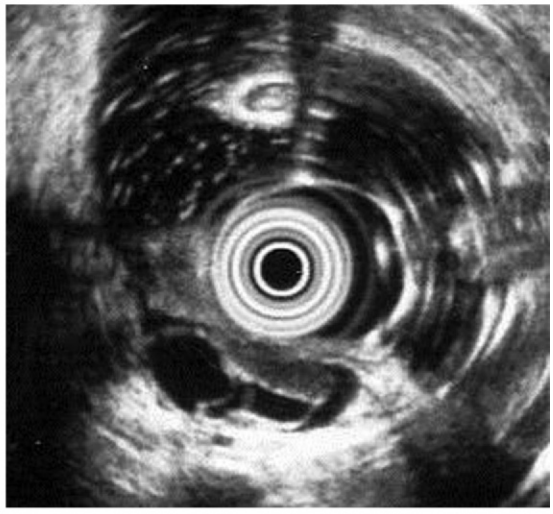

c.

**Figure 19.** Tailgut cyst. **(a)** Axial T2-weighted MR image shows a hyperintense multilocular cystic mass. **(b)** Axial contrast-enhanced T1-weighted MR image shows a thin rim of peripheral enhancement around the mass. **(c)** Endoscopic US image shows that the cystic areas are anechoic, with increased through-transmission and thin internal septa.

infected, they tend to be thick-walled with surrounding inflammatory change, and they may contain air if a fistula is present. Typically, developmental cysts are hypointense on T1-weighted MR images, although they may be hyperintense if they contain mucoid material, and hyperintense on T2-weighted images. Focal irregular wall thickening with enhancement is suggestive of malignant degeneration. Traditionally, treatment consisted of complete surgical excision because of the risk of recurrence, malignant degeneration, and chronic infection (29). However, given the increased rate of detection of incidental benign lesions at cross-sectional imaging, some patients with developmental cysts are monitored without undergoing surgery.

## Germ Cell Tumors

Germ cell tumors occur secondary to disorganization of totipotent primitive neural cells during embryogenesis. The degree of differentiation determines the tumor type, with teratomas, yolk sac tumors, and embryonal cell carcinomas demonstrating lower degrees of differentiation (3). Sacrococcygeal teratoma is the most common presacral germ cell tumor in children and the most common solid tumor in neonates, with a prevalence of one in 35,000–40,000 births. Sacrococcygeal teratomas are three to four times more common in girls, and 60% of tumors are benign (3,31).

Patients with a sacrococcygeal teratoma present with a presacral or pelvic mass that ranges from predominantly external to completely internal at rectal examination; approximately 50% of tumors are predominantly external (3). Less than 10% of tumors are diagnosed in patients who are over 2 years old. Those that are diagnosed in patients who are over 2 years old are predominantly

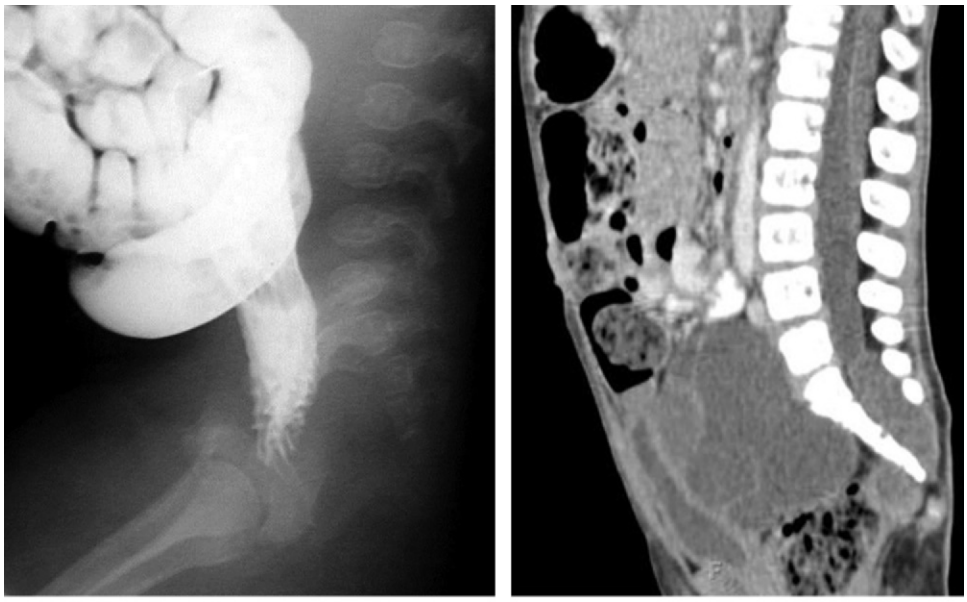

a. c.

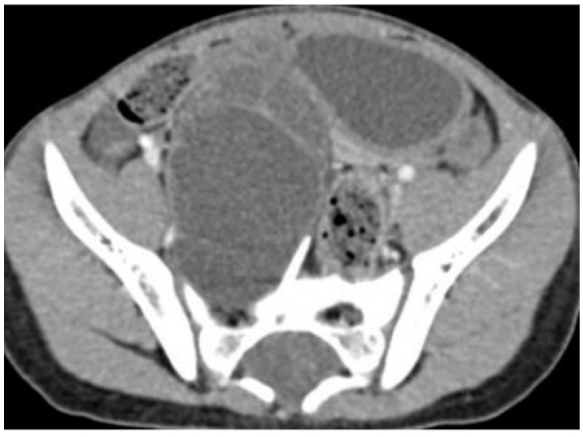

b.

**Figure 20.** Sacrococcygeal teratoma in two patients. **(a)** Image from a barium enema study shows widening of the presacral space. **(b, c)** Axial **(b)** and sagittal **(c)** contrast-enhanced CT images in another patient show a large multiloculated solid and cystic mass that extends into the sacral canal and foramina. Associated bone remodeling and destruction are seen.

internal, with intrapelvic and abdominal components. Masses that are predominantly internal are most likely to be malignant (38% of such cases are malignant).

The imaging features of teratomas depend on their contents (3). Benign teratomas contain only mature tissues, including fluid, fat, calcification, and a small amount of soft tissue. Benign teratomas are predominantly cystic, with fluid attenuation at CT. Areas of bone, fat, and calcification may be seen. At T1-weighted MR imaging, areas that contain fat have high signal intensity, and those that contain bone and calcifications demonstrate signal voids. On images obtained during barium enema study, the colon and rectum are anteriorly displaced by tumor (Fig 20). The coccyx is always involved by teratoma and is resected along with the tumor. Malignant tumors have more solid tissue than benign tumors, with areas of hemorrhage and necrosis common.

Yolk sac tumors have a more aggressive imaging appearance than teratomas and are characterized by more heterogeneous soft tissues and areas of hemorrhage and necrosis (32). At CT, areas of low attenuation with no enhancement are seen, and at T1-weightd MR imaging, areas of hyperintensity are seen, a finding related to hemorrhage (Fig 21). Yolk sac tumors demonstrate heterogeneous contrast enhancement and often invade adjacent organs.

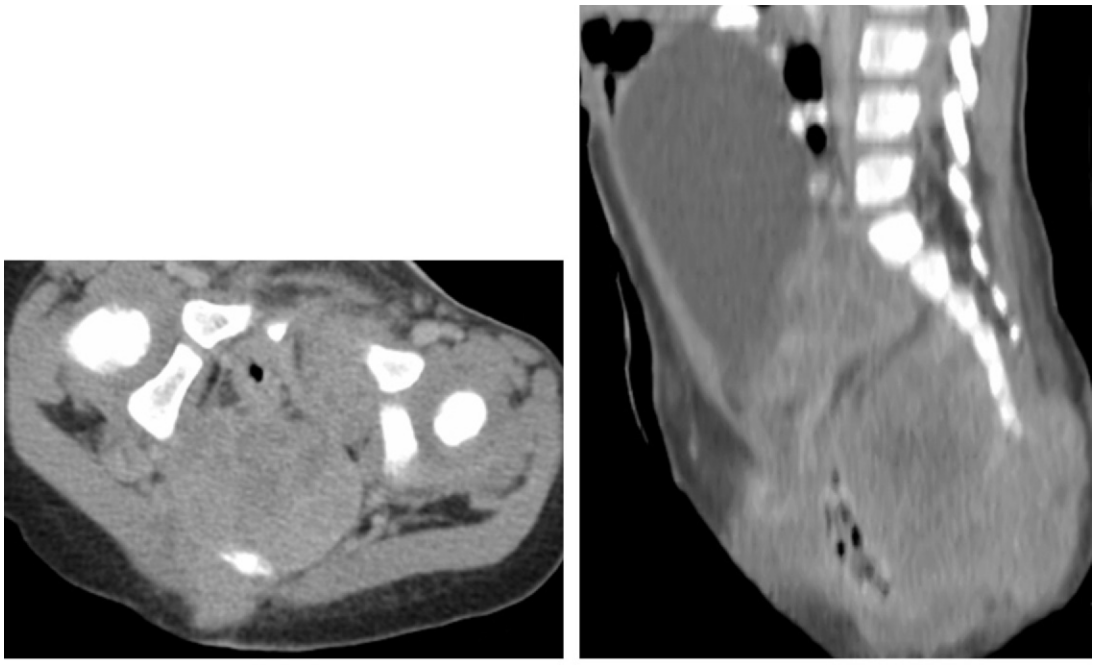

a. b.

**Figure 21.** Yolk sac tumor. Axial **(a)** and sagittal **(b)** contrast-enhanced CT images show a heterogeneously enhancing presacral mass that extends into the sacral canal.

Treatment of germ cell tumors consists of surgical excision of both tumor and coccyx (25). Failure to completely resect the coccyx is associated with a high rate of recurrence. Patients with a malignant germ cell tumor undergo additional chemo- or radiation therapy. Incomplete surgical resection due to invasion of adjacent structures or the presence of metastatic disease indicates a poor prognosis.

## Other Conditions

Infectious, inflammatory, and posttraumatic conditions may cause space-occupying, mass-like lesions to form in the presacral space. Such lesions should be considered part of a comprehensive differential diagnosis. For instance, in patients with severe diskitis or osteomyelitis, a large prevertebral abscess may extend into the presacral space, and pelvic trauma may lead to hematomas that extend into the presacral space. These entities may be diagnosed on the basis of characteristic imaging features in the appropriate clinical setting: Presacral abscesses demonstrate an enhancing rim, and hematomas demonstrate an area of high attenuation at CT.

## Conclusions

The presacral space is a clinically important space that is relevant to multiple disciplines and is affected by a wide variety of benign and malignant conditions. An appropriate differential diagnosis may be formulated from a more comprehensive list by considering the specific imaging features of a given case.

***Disclosures of Conflicts of Interest*.—P.J.P.:** *Related financial activities:* none. *Other financial activities:* consultant for Viatronix, Check-Cap, Bracco, and iCAD.

## References


1. Ghosh J, Eglinton T, Frizelle FA, Watson AJ. Presacral tumours in adults. Surgeon 2007;5(1):31–38.
2. Wolpert A, Beer-Gabel M, Lifschitz O, Zbar AP. The management of presacral masses in the adult. Tech Coloproctol 2002;6(1):43–49.
3. Kocaoglu M, Frush DP. Pediatric presacral masses. RadioGraphics 2006;26(3):833–857.
4. Diel J, Ortiz O, Losada RA, Price DB, Hayt MW, Katz DS. The sacrum: pathologic spectrum, multimodality imaging, and subspecialty approach. RadioGraphics 2001;21(1):83–104.
5. Murphey MD, Andrews CL, Flemming DJ, Temple HT, Smith WS, Smirniotopoulos JG. Primary tumors of the spine: radiologic-pathologic correlation. RadioGraphics 1996;16(5):1131–1158.
6. Randall RL. Giant cell tumor of the sacrum. Neurosurg Focus 2003;15(2):E13.
7. Kaplan PA, Murphey M, Greenway G, Resnick D, Sartoris DJ, Harms S. Fluid-fluid levels in giant cell tumors of bone: report of two cases. J Comput Tomogr 1987;11(2):151–155.
8. Bass JC, Korobkin M, Francis IR, Ellis JH, Cohan RH. Retroperitoneal plexiform neurofibromas: CT findings. AJR Am J Roentgenol 1994;163(3):617–620.
9. Paulsen RD, Call GA, Murtagh FR. Prevalence and percutaneous drainage of cysts of the sacral nerve root sheath (Tarlov cysts). AJNR Am J Neuroradiol 1994;15(2):293–297; discussion 298–299.
10. Ha HI, Seo JB, Lee SH, et al. Imaging of Marfan syndrome: multisystemic manifestations. RadioGraphics 2007;27(4):989–1004.
11. Villarejo F, Scavone C, Blazquez MG, et al. Anterior sacral meningocele: review of the literature. Surg Neurol 1983;19(1):57–71.
12. Koeller KK, Rosenblum RS, Morrison AL. Neoplasms of the spinal cord and filum terminale: radiologic-pathologic correlation. RadioGraphics 2000;20(6):1721–1749.
13. Bethke KP, Neifeld JP, Lawrence W Jr. Diagnosis and management of sacrococcygeal chordoma. J Surg Oncol 1991;48(4):232–238.
14. Fourney DR, Gokaslan ZL. Current management of sacral chordoma. Neurosurg Focus 2003;15(2):E9.
15. Vilanova JC, Barceló J, Smirniotopoulos JG, et al. Hemangioma from head to toe: MR imaging with pathologic correlation. RadioGraphics 2004;24(2):367–385.
16. Dubois J, Garel L. Imaging and therapeutic approach of hemangiomas and vascular malformations in the pediatric age group. Pediatr Radiol 1999;29(12):879–893.
17. Rao P, Kenney PJ, Wagner BJ, Davidson AJ. Imaging and pathologic features of myelolipoma. RadioGraphics 1997;17(6):1373–1385.
18. Shanbhogue AK, Prasad SR, Takahashi N, Vikram R, Zaheer A, Sandrasegaran K. Somatic and visceral solitary fibrous tumors in the abdomen and pelvis: cross-sectional imaging spectrum. RadioGraphics 2011;31(2):393–408.
19. Park SB, Park YS, Kim JK, et al. Solitary fibrous tumor of the genitourinary tract. AJR Am J Roentgenol 2011;196(2):W132–W137.
20. Bonekamp D, Horton KM, Hruban RH, Fishman EK. Castleman disease: the great mimic. RadioGraphics 2011;31(6):1793–1807.
21. Pickhardt PJ, Bhalla S. Unusual nonneoplastic peritoneal and subperitoneal conditions: CT findings. RadioGraphics 2005;25(3):719–730.
22. Amis ES Jr. Retroperitoneal fibrosis. AJR Am J Roentgenol 1991;157(2):321–329.
23. Lucey BC, Stuhlfaut JW, Soto JA. Mesenteric lymph nodes seen at imaging: causes and significance. RadioGraphics 2005;25(2):351–365.
24. Levy AD, Remotti HE, Thompson WM, Sobin LH, Miettinen M. Gastrointestinal stromal tumors: radiologic features with pathologic correlation. RadioGraphics 2003;23(2):283–304, 456; quiz 532.
25. Wells RG, Sty JR. Imaging of sacrococcygeal germ cell tumors. RadioGraphics 1990;10(4):701–713.
26. Metser U, You J, McSweeney S, Freeman M, Hendler A. Assessment of tumor recurrence in patients with colorectal cancer and elevated carcinoembryonic antigen level: FDG PET/CT versus contrast-enhanced 64-MDCT of the chest and abdomen. AJR Am J Roentgenol 2010;194(3):766–771.
27. Pickhardt PJ, Bhalla S. Primary neoplasms of peritoneal and sub-peritoneal origin: CT findings. RadioGraphics 2005;25(4):983–995.
28. Pickhardt PJ, Fisher AJ, Balfe DM, Dehner LP, Huettner PC. Desmoplastic small round cell tumor of the abdomen: radiologic-histopathologic correlation. Radiology 1999;210(3):633–638.
29. Dahan H, Arrivé L, Wendum D, Docou le Pointe H, Djouhri H, Tubiana JM. Retrorectal developmental cysts in adults: clinical and radiologic-histopathologic review, differential diagnosis, and treatment. RadioGraphics 2001;21(3):575–584.
30. Lev-Chelouche D, Gutman M, Goldman G, et al. Presacral tumors: a practical classification and treatment of a unique and heterogeneous group of diseases. Surgery 2003;133(5):473–478.
31. Keslar PJ, Buck JL, Suarez ES. Germ cell tumors of the sacrococcygeal region: radiologic-pathologic correlation. RadioGraphics 1994;14(3):607–620; quiz 621–622.
32. Ueno T, Tanaka YO, Nagata M, et al. Spectrum of germ cell tumors: from head to toe. RadioGraphics 2004;24(2):387–404.

# Presacral Masses: Multimodality Imaging of a Multidisciplinary Space

*Kendra S. Hain, MD • Perry J. Pickhardt, MD • Meghan G. Lubner, MD • Christine O. Menias, MD • Sanjeev Bhalla, MD*

**RadioGraphics 2013;** 33:1145–1167 • **Published online** 10.1148/rg.334115171 • **Content Codes:** GI GN GU MR

**Page 1153**
The mortality rate in patients who do not undergo surgery is 30%, a result of pelvic obstruction at the time of labor in childbearing women or erosion into the rectum, followed by meningitis in men and women of all ages.

**Page 1154**
Hemorrhage is common, and a low-signal-intensity rim (the cap sign) may be seen. Intense enhancement is seen on contrast-enhanced images, and flow voids are common.

**Pages 1156**
Extra-adrenal myelolipomas most commonly occur in the retroperitoneum, but they may also be found in the chest or pelvis.

**Page 1157**
Solitary fibrous tumors may occur anywhere in the body. It was recently established that extrapleural tumors are more common than pleural tumors.

**Page 1163**
However, tailgut cysts are the most common asymptomatic presacral lesions that are incidentally found in adults.